Tunneling conductivity in composites of attractive colloids

B. Nigro, C. Grimaldi, M. A. Miller, P. Ryser, and T. Schilling

Citation: J. Chem. Phys. **136**, 164903 (2012); doi: 10.1063/1.4705307
View online: http://dx.doi.org/10.1063/1.4705307
View Table of Contents: http://jcp.aip.org/resource/1/JCPSA6/v136/i16
Published by the AIP Publishing LLC.

Tunneling conductivity in composites of attractive colloids

B. Nigro,[1,a)] C. Grimaldi,[1,b)] M. A. Miller,[2] P. Ryser,[1] and T. Schilling[3]
[1]*LPM, Ecole Polytechnique Fédérale de Lausanne, Station 17, CP-1015 Lausanne, Switzerland*
[2]*University Chemical Laboratory, Lensfield Road, Cambridge CB2 1EW, United Kingdom*
[3]*Université du Luxembourg, 162 A, Avenue de la Faïencerie L-1511, Luxembourg*

(Received 27 February 2012; accepted 5 April 2012; published online 25 April 2012)

In conductor-insulator nanocomposites in which conducting fillers are dispersed in an insulating matrix, the electrical connectedness is established by inter-particle tunneling or hopping processes. These systems are intrinsically non-percolative and a coherent description of the functional dependence of the conductivity σ on the filler properties, and in particular of the conductor-insulator transition, requires going beyond the usual continuum percolation approach by relaxing the constraint of a fixed connectivity distance. In this article, we consider dispersions of conducting spherical particles which are connected to all others by tunneling conductances and which are subjected to an effective attractive square-well potential. We show that the conductor-insulator transition at low contents ϕ of the conducting fillers does not determine the behavior of σ at larger concentrations, in striking contrast to what is predicted by percolation theory. In particular, we find that at low ϕ the conductivity is governed almost entirely by the stickiness of the attraction, while at larger ϕ values σ depends mainly on the depth of the potential well. As a consequence, by varying the range and depth of the potential while keeping the stickiness fixed, composites with similar conductor-insulator transitions may display conductivity variations of several orders of magnitude at intermediate and large ϕ values. By using a recently developed effective medium theory and the critical path approximation, we explain this behavior in terms of dominant tunneling processes which involve inter-particle distances spanning different regions of the square-well fluid structure as ϕ is varied. Our predictions could be tested in experiments by changing the potential profile with different depletants in polymer nanocomposites. © *2012 American Institute of Physics*. [http://dx.doi.org/10.1063/1.4705307]

I. INTRODUCTION

The challenge of understanding the electrical transport properties in conductor-insulator composites is central for conceiving and designing new composite materials with unique electrical properties, and has fueled ongoing research ranging from fundamental statistical physics to the more applied materials science and nanotechnology. In this respect, recent years have seen remarkable progress in the design and synthesis of polymer nanocomposites with controllable structural parameters, so as to combine advantageous properties of the insulating polymer matrix (flexibility, light weight, transparency, etc.) with appropriate levels of electrical conductivity σ. For example, high aspect ratio conducting fillers, such as carbon fibers and nanotubes, graphite platelets, and graphene sheets, as well as segregated dispersions of carbon-black particles, have been shown to reduce strongly the loadings ϕ needed to achieve conducting composites.[1–3] The interplay of multicomponent fillers has been recently demonstrated to have a strong influence on transport properties.[4] Other studies have evidenced the role of depletants[5] and of shear forces[6] in the formation and structure of the conducting network of carbon nanotubes, thus underlining the importance of the coupling between the conducting and insulating phases,[7] and how this can be used to tune the overall composite conductivity.

On the theoretical side, the general understanding of the effects of the filler properties on σ has been traditionally based on the continuum percolation theory of transport. The premise behind this approach is that there exists a fixed inter-particle distance beyond which two particles are electrically disconnected, thereby leading to a well-defined percolation threshold ϕ_c for the connected particles which marks the transition between the conducting (at $\phi > \phi_c$) and the insulating (at $\phi < \phi_c$) regimes of the composite.[8,9] In the vicinity of ϕ_c, the resulting percolation conductivity is thus predicted to follow the power-law relation

$$\sigma_{\text{perc}} \simeq \sigma^0_{\text{perc}}(\phi - \phi_c)^t, \tag{1}$$

where $t \simeq 2$ is the universal transport exponent for three-dimensional percolating systems. Equation (1) is customarily used to interpret the ϕ-induced conductor-insulator transition observed in real composite materials, which are thus viewed as truly percolating systems, although the values of t extracted from experiments often deviate from universality.[1,10] Due to the percolation hypothesis, most theoretical efforts have been concentrated on the calculation of the percolation threshold ϕ_c and of its dependencies on the filler particle shapes,[11–13] dispersions,[14,15] and filler-filler and filler-matrix interactions.[16–19]

In polymer nanocomposites, or more generally in colloidal-like dispersions of conducting fillers in insulating matrices, the electron transfer between particles is mediated by tunneling or hopping processes, which implies that the

a)biagio.nigro@epfl.ch.
b)claudio.grimaldi@epfl.ch.

conductance between any two particles decays continuously with the inter-particle distance [see Eq. (4) below]. In this case, no fixed connectivity length can be unambiguously identified and, consequently, the premise for the existence of a percolation transition, and for the validity of Eq. (1), is unjustified for this class of composites. This poses the problem of understanding the observed filler dependencies of σ without relying on the percolation hypothesis.

Recently, the problem of finding the functional dependence of σ for colloidal composites without imposing any *a priori* fixed connectivity distance has been tackled by considering explicitly the electron tunneling conduction between any two particles in the composite.[20–22] One important outcome was the realization that, despite the absence of a real percolation threshold, the transition from the conducting to the insulating regimes could still be characterized by a characteristic concentration ϕ_p below which σ is dominated by the (small but finite) conductivity σ_p of the insulating matrix. In particular, by considering equilibrium dispersions of hard spheroidal particles, ϕ_p was shown to decrease with the particle aspect ratio,[20] in accord with the general trend observed in composites with fibrous and plate-like fillers.

In this article, we study by theory and simulations the functional dependence of σ when, in addition to steric interactions, the conducting colloidal particles are subjected to mutual attraction modeled by a square-well potential. We show that attraction, when combined with tunneling, gives rise to unexpected features which could not be anticipated by the usual continuum percolation theory. Specifically, we find that the range and the depth of the attraction affect the conductivity in very different ways according to whether ϕ is small or large. In particular, the low-ϕ behavior of σ, and so the crossover ϕ_p to the insulating regime, turns out to be almost entirely governed by the overall stickiness of the attraction, while the conductivity at $\phi > \phi_p$ is found to change by several orders of magnitude for different potential profiles even if the stickiness is kept constant. This kind of behavior is completely missed if the conductor-insulator crossover is treated as a true percolation transition occurring at the critical concentration ϕ_c, because in this case the ϕ dependence of the percolation conductivity $\sigma_{\rm perc}$ of Eq. (1) is basically determined by ϕ_c alone.

As shown in the following, in which a recently developed effective medium theory and the critical path approximation (CPA) are used to interpret the simulation results, the effects of the attractive potential on σ can be rationalized in terms of a ϕ-dependent dominant distance between the fillers which governs the composite conductivity. This correspondence establishes a direct connection between the functional dependence of σ and the structure of the square-well fluid, which could be in principle exploited in the synthesis of real nanocomposite materials with optimized conduction characteristics.

II. MODEL

Attractive forces between filler particles in polymer nanocomposites may arise from several mechanisms such as van der Waals forces or depletion interactions induced by non-adsorbing polymers or surfactant micelles.[23] In the latter case, the size and concentration of the depletants control, respectively, the range and depth of the attractive interaction, which can be modeled by a suitable effective potential. Here, we represent the conducting fillers by hard-core spheres of diameter D and for any two spheres centered at $\mathbf{r}_i$ and $\mathbf{r}_j$, we model the attraction by a square-well potential $u(r_{ij})$ of the form

$$u(r_{ij}) = \begin{cases} +\infty & \text{for } r_{ij} \le D, \\ -\epsilon & \text{for } D < r_{ij} \le \lambda D, \\ 0 & \text{for } r_{ij} > \lambda D, \end{cases} \tag{2}$$

where $r_{ij} = |\mathbf{r}_i - \mathbf{r}_j|$ and λD ($\lambda \ge 1$) is the range of attraction. In the following, we shall vary both λ and ϵ so as to consider the hard sphere (HS) case ($\epsilon = 0$), the short-range attraction regime $\epsilon \neq 0$ and $\lambda \le 1.25$, and the adhesive hard sphere (AHS) limit,[24] which is obtained by taking $\lambda \to 1$ and $\epsilon \to \infty$ with

$$\tau = \frac{\lambda \exp(-\epsilon^*)}{12(\lambda - 1)} \tag{3}$$

constant, where $\epsilon^* = \epsilon/kT$ and kT is the thermal energy. τ is an inverse measure of particle stickiness which governs, together with the concentration, the phase behavior of short-range square-well fluids.[25,26] In the following, we limit our study to values of τ above the critical point for gas-liquid-like phase separation.[27]

We describe the electron transport processes by considering each sphere as being electrically connected to all others through inter-particle tunneling conductances of the form

$$g(r_{ij}) = g_0 \exp\left[-\frac{2(r_{ij} - D)}{\xi}\right], \tag{4}$$

where ξ is the tunneling decay length, which is independent of the range of the attraction λ. In writing Eq. (4), we assume that the size D of the conducting particle and the temperature are large enough to neglect charging energy effects and Coulomb interactions. Furthermore, we have ignored any dependence on r_{ij} of the prefactor g_0, which we set equal to 1.

III. NUMERICAL RESULTS FOR THE CONDUCTIVITY

We performed standard metropolis Monte Carlo (MC) simulations to find equilibrium dispersions of $N = 2000$ particles in a cubic box of side length L, which was changed to obtain different values of the volume fraction $\phi = \pi N D^3/6L^3$. A dedicated Monte Carlo algorithm[28] was used for the AHS limit. For all the ϕ values considered and for each potential profile, we obtained $N_R = 300$ independent equilibrium configurations of the system.

To obtain the composite conductivity σ, we constructed for each of the N_R configurations a tunneling resistor network with inter-particle conductances $g(r_{ij})$ given by Eq. (4). In order to reduce computational times, we exploited the exponential decay of Eq. (4) by neglecting contributions from particles sufficiently far apart so as to reduce the number of connected particles in the network. To this end, we introduced an adjustable cut-off length $\delta_{\rm max}$ such that the bond conductances for $\delta_{ij} > \delta_{\rm max}$ can be safely removed from the network without altering σ.[20,22] Finally, we solved this reduced network

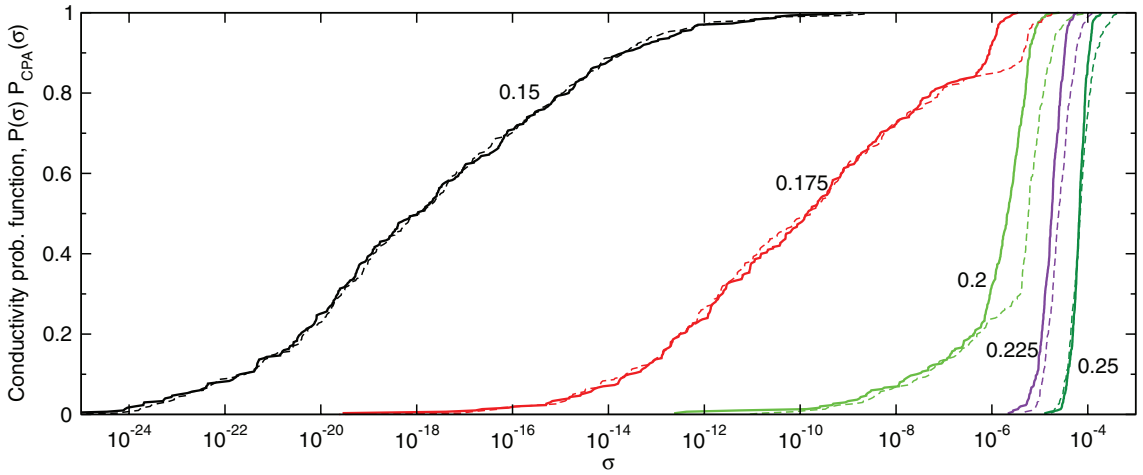

FIG. 1. Conductivity probability function $P(\sigma)$ (thick solid lines) for various values of the volume fraction ϕ and for a square-well potential with $\lambda = 1.05$ and $\tau = 0.2$. Here, the tunneling factor is $\xi/D = 0.01$ and the number of conducting spheres is fixed at $N = 2000$. The thin dashed lines are the $P_{\rm CPA}(\sigma)$ curves obtained from $P(\delta)$ of Fig. 6 and by using $\sigma = \sigma_0 \exp(-2\delta/\xi)$ with $\sigma_0 = 0.09$.

using a combination of numerical decimation and preconditioned conjugate gradient algorithms as described in Ref. 22. From the resulting network conductance G, the dimensionless conductivity σ follows from $\sigma = GD/L$.

In Fig. 1, we show some representative examples of the cumulative distribution function (CDF) $P(\sigma)$ of the conductivity (thick solid lines) obtained from all N_R realizations of the network for $\lambda = 1.05$, $\tau = 0.2$, and for different values of the volume fraction ϕ. In all cases, the tunneling decay length has been set equal to $\xi/D = 0.01$. Overall, the rise from 0 to 1 of $P(\sigma)$ becomes more gradual as ϕ decreases, which comes from keeping the number of particles N fixed. Additionally, for $\phi = 0.175$ and 0.2 the CDF displays a sudden increase at $\sigma \simeq 0.5 \times 10^{-7}$. As discussed in more detail in Sec. V, this latter feature can be traced back to the discontinuity of the radial distribution function (RDF) of the square-well fluid at inter-particle distances $r = \lambda D$. Since the numerical procedure for solving the tunneling network is rather time consuming, we have not attempted to study finite size-effects on $P(\sigma)$ systematically. Instead, we have chosen to extract the overall network conductivity from the condition $P(\sigma) = 1/2$ applied to the CDF computed for $N = 2000$. As shown in Sec. V, where we study the conductivity within the critical path approximation for which a finite-size analysis is feasible, this criterion provides a robust estimate of the conductivity for infinite systems.

In the main panels of Fig. 2, we show the network conductivity σ (open symbols) as a function of ϕ for $\xi/D = 0.01$ and for different parameters λ and ϵ^* of the square-well potential. For comparison, the HS limit is plotted in Fig. 2(a) as open squares. By inspection of the two panels of the figure, we see that the ϕ-dependence of σ strongly depends on the way in which the potential profile is changed. Namely, in Fig. 2(a) the conductivity is steadily enhanced for all

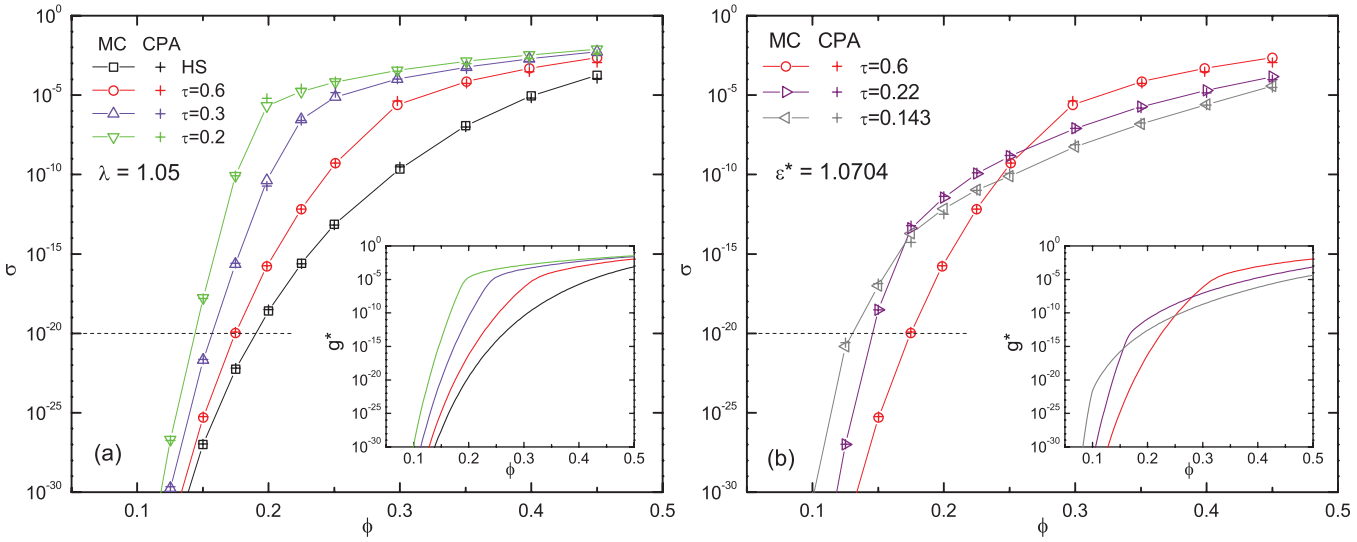

FIG. 2. Network conductivity σ as a function of the volume fraction ϕ obtained from MC calculations (open symbols) and from CPA (plus signs). (a) σ for well range fixed at $\lambda = 1.05$ and different well depths ϵ^* parametrized by τ of Eq. (3). (b) σ for well depth fixed at $\epsilon^* = 1.0704$ and $\lambda = 1.05$, 1.15, and 1.25. Insets: corresponding EMA conductance g^*.

ϕ values when the well depth is increased while keeping the range parameter fixed at $\lambda = 1.05$, leading for example at $\phi = 0.25$ to an enhancement of up to 9 orders of magnitude compared to the HS limit. Conversely, as shown in Fig. 2(b), when the potential depth is kept as fixed ($\epsilon^* = 1.0704$) but its range varies from $\lambda = 1.05$ to $\lambda = 1.25$ the conductivity at low ϕ is enhanced, while at intermediate and large ϕ it is diminished by about three orders of magnitude.

The different functional dependencies of σ in Figs. 2(a) and 2(b) have important consequences in conjunction with the conductor-insulator transition of composites. Indeed, although we have considered conducting particles dispersed in a perfectly insulating medium, in real polymer composites the conductivity σ_p of the polymeric matrix is small but finite at nonzero temperatures, being typically 10^{-13}–10^{-18} S/cm at room temperature. Hence, despite the fact that the tunneling conductivity drops all the way to zero as $\phi \to 0$, the conductivity of the complete system (particles and polymer) is limited from below by σ_p.[29] One can thus identify a crossover point separating tunneling-dominated from polymer-dominated conductivity with the volume fraction ϕ_p below which σ matches that of the polymer matrix, as is generally done in the analysis of experimental conductivity data of real nanocomposites. As schematically shown in the main panels of Fig. 2, where the horizontal dashed line represents σ_p fixed for illustrative purposes at 10^{-20}, we can estimate ϕ_p as the intersection point between the calculated tunneling conductivity and σ_p.[20] In this way, we find that as the stickiness of the square-well is enhanced (i.e., τ is diminished) ϕ_p is systematically lowered. However, it is evident by comparing Fig. 2(a) with Fig. 2(b), that the behavior of σ in the conducting regime $\phi > \phi_p$ is not determined by ϕ_p alone. For example, the curves for $\tau = 0.2$ in Fig. 2(a) and for $\tau = 0.22$ in Fig. 2(b) have similar ϕ_p but very different conductivities at larger ϕ.

This latter feature is illustrated even more strikingly in Fig. 3 where σ is plotted for different values of ϵ^* and λ such that the stickiness parameter τ remains constant. Even though ϕ_p is basically unchanged in going from $\lambda = 1.25$ to the AHS limit at $\lambda = 1$, the conductivity increases by 5 to 10 orders of magnitude above the HS case at fixed ϕ in the whole $\phi > \phi_p$ range. Note that a similar behavior is also found if we change the value of σ_p provided that it remains sufficiently small. For example, if in Fig. 3 we consider $\sigma_p = 10^{-15}$, the curves for $\lambda \leq 1.15$ would still have equal ϕ_p, though slightly larger than the previous case but very different σ at larger ϕ.

Our general observation that in square-well fluids of conducting spheres the conductivity for $\phi > \phi_p$ is not determined by the position of the conductor-insulator crossover is in striking contrast with the usual continuum percolation description. Indeed, if the conductor-insulator transition is viewed as a true percolation transition, then the corresponding conductivity would follow Eq. (1) for $\phi \gtrsim \phi_c$, where ϕ_c is the percolation threshold, and so the conductivity level in the conducting regime would be completely determined by ϕ_c. For the short-range potentials considered here ϕ_c is known to be reduced by enhanced stickiness,[17] in line with the behavior of ϕ_p, and consequently, from Eq. (1), the percolation conductivity for $\phi \gtrsim \phi_c$ would also be systematically enhanced. Conversely, different potentials with the same parameter τ would give similar percolation conductivity curves, in strong disagreement with our results of Fig. 3.

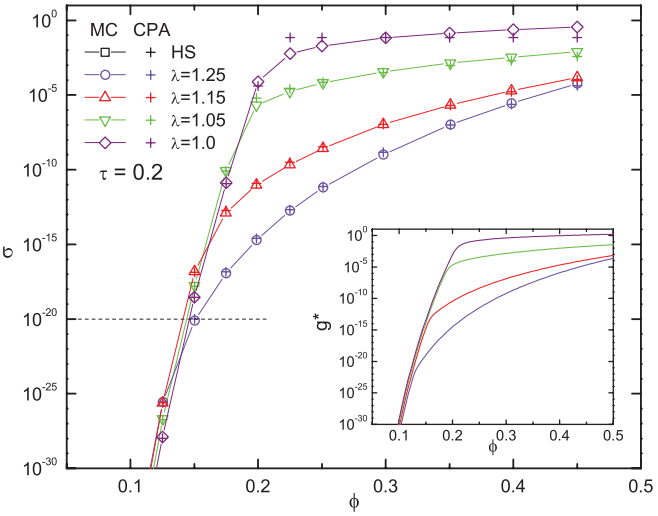

FIG. 3. Network conductivity σ as a function of ϕ obtained from MC calculations (open symbols) and from CPA (plus signs) for different well widths and depths with fixed $\tau = 0.2$. Inset: corresponding EMA conductance g^*.

The results shown in Figs. 2 and 3 also have important practical consequences in relation to the problem of controlling the conductivity of polymer nanocomposites by tuning the attraction through, for example, the depletion interaction.[5] Indeed, from Figs. 2 and 3, it turns out that the best strategy to obtain high levels of conductivity for a broader range of filler concentrations is by choosing potential profiles that are very deep and short-ranged (but of course not strong enough to induce phase separation). For depletion induced attraction, this corresponds to having a large concentration of depletants with small sizes compared to those of the conducting particles.

We conclude this section by addressing the role of the tunneling decay length ξ in the overall functional dependence of σ. In Fig. 4, we plot σ for $\tau = 0.2$ and $\lambda = 1.05$ in units

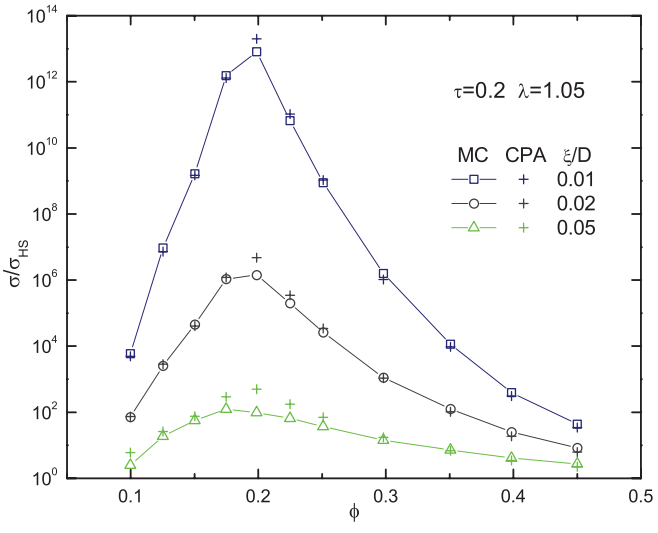

FIG. 4. Enhancement factor of the conductivity for $\tau = 0.2$ compared to the conductivity in the HS limit for different values of the tunneling length ξ/D.

of the HS conductivity for $\xi/D = 0.01$, 0.02, and 0.05. As expected, the strong enhancement obtained for $\xi/D = 0.01$ is systematically reduced as ξ/D increases. For example, at $\xi/D = 0.05$ only a maximum 10^2 fold enhancement with respect to the HS limit is achieved. This is because for large ξ/D, two particles having separation less or greater than the potential range have similar tunneling probabilities, and so the short-range structure of the square-well fluid is smeared out. If we consider that, depending on the material properties, the tunneling decay length ranges from a fraction of a nanometer to a few nanometers, from the results of Fig. 3 we expect that particle sizes of tens to hundreds of nanometers are optimal for σ to be strongly enhanced by increased attraction.

IV. EFFECTIVE MEDIUM THEORY

The numerical results of Sec. III and the effects of attraction on the functional dependence of σ find a more complete understanding by employing the effective medium approximation (EMA) introduced in Refs. 21 and 30. Briefly, this EMA amounts to replacing each conductance $g(r_{ij})$ of Eq. (4) by an effective value, $\bar{g}$, which is independent of the interparticle distance r_{ij}. By requiring that the resulting effective and fully connected network has the same average resistance as the original, and by considering only two-site clusters,[30] the following self-consistent equation is found[21,30]

$$24\phi \int_0^\infty dx\, x^2 g_2(x) \left[\frac{1}{g^* \exp[2D(x-1)/\xi] + 1} \right] = 2, \tag{5}$$

where $x = r/D$, $g_2(x)$ is the RDF for the conducting spheres, and $g^* = N\bar{g}/2$ is the two-point conductance of the effective N-node network.

We have numerically solved Eq. (5) for g^* using the quasi-analytical model RDF proposed in Ref. 31 for the square-well fluid, which reduces to the Percus-Yevick approximation for both the HS and AHS limits and is in rather good agreement with the MC results of the RDF for $\lambda < 1.3$.[31,32] Although g^* is a two-point conductance (which is the meaningful quantity for a complete network of identical resistors) rather than a conductivity, the EMA results shown in the insets of Figs. 2 and 3 and in Fig. 5 (solid lines) closely follow the conductivity behavior obtained by the full numerical solution of the tunneling network. Using Eq. (5), we can thus explain the effect of attraction on σ by reasoning simply in terms of $g_2(x)$ and of its dependence on the square-well potential. To this end, let us rewrite the EMA conductance as

$$g^* = \exp[-2D(x^* - 1)/\xi], \tag{6}$$

where we have introduced a characteristic EMA distance x^*. By noting that for $\xi/D \ll 1$ the term in square brackets in Eq. (5) reduces to the step function $\theta(x^* - x)$, x^* is found as the solution of the following equation:

$$24\phi \int_0^{x^*} dx\, x^2 g_2(x) = 2, \tag{7}$$

where the left hand side gives the number of particle centers having distances less than x^* from a particle at the origin. To proceed further, we note that for sufficiently narrow and deep potential wells the RDF can be approximated by

$$g_2(x) = \theta(x-1)[g_2(1^+)\theta(\lambda - x) + 1], \tag{8}$$

where $g_2(1^+)$ is the RDF at contact, and from Eq. (7) we obtain finally

$$x^* = \begin{cases} \left[\dfrac{1}{4\phi g_2(1^+)} + 1 \right]^{1/3} & \text{for } x^* < \lambda, \\ \left[\dfrac{1}{4\phi} - g_2(1^+)(\lambda^3 - 1) + \lambda^3 \right]^{1/3} & \text{for } x^* > \lambda. \end{cases} \tag{9}$$

As shown in Fig. 5, g^* obtained from Eqs. (6) and (9) (dashed lines) is in overall good agreement with the solutions of Eq. (5) with the full RDF of Ref. 31. Furthermore, Eq. (9) explicitly introduces two different regimes according to whether the EMA distance x^* is less or greater than λ, which physically corresponds to whether the dominant tunneling processes occur between particles with separation less or greater than the well range. The two regimes $x^* > \lambda$ and $x^* < \lambda$ identify two different regions, respectively, $\phi < \phi^*$ and $\phi > \phi^*$, where ϕ^* is a characteristic concentration (not to be confused with ϕ_p) obtained from the condition $x^* = \lambda$ applied

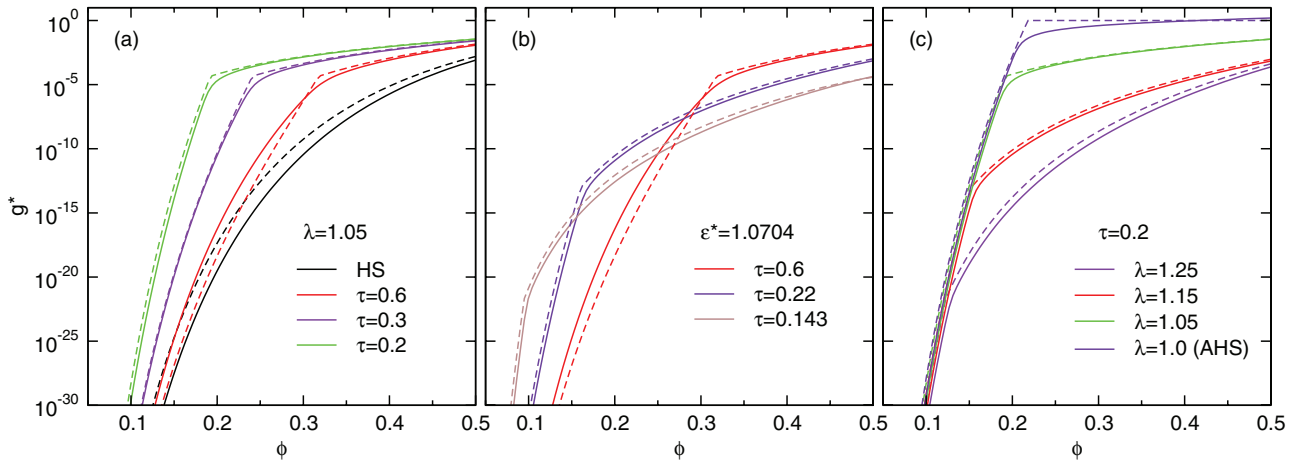

FIG. 5. Comparison between the full numerical solution of the EMA Eq. (5) (solid lines) and g^* obtained from Eqs. (6) and (9) (dashed lines). The parameters used in (a), (b), and (c) are the same of those in Figs. 2(a), 2(b), and 3, respectively.

to Eq. (9), i.e., $4\phi^* g_2(1^+)(\lambda^3 - 1) = 1$. Since $g_2(1^+)$ scales essentially as $\exp(\epsilon^*)$,[31] ϕ^* can be approximated by τ/λ^2 for $\lambda - 1$ and τ small.

From Eq. (9) and $g_2(1^+) \approx \exp(\epsilon^*)$, we thus see that the conduction at large densities ($\phi > \phi^*$) is mainly governed by the well depth, which is indeed expected since in this regime $x^* < \lambda$. In contrast, from Eq. (9), g^* turns out to be affected by both ϵ^* and λ at low densities ($\phi < \phi^*$) because the relevant tunneling distances span the entire well range (i.e., $x^* > \lambda$). In this regime and for sufficiently narrow wells, $g_2(1^+)(\lambda^3 - 1) - \lambda^3$ reduces simply to $1/4\tau - 1 + \mathcal{O}([\lambda - 1]/\tau)$, which explains the equal asymptotic behaviors for $\phi \to 0$ of Fig. 3 as ϵ^* and λ are changed but τ is held fixed.

From the low-density approximation derived above, it is also possible to deduce the conductor-insulator crossover point ϕ_p by introducing a two-point conductance $g_p \ll 1$ of the polymeric matrix, which represents the EMA equivalent of σ_p introduced in Sec. III. Thus, by requiring that Eq. (6) coincides with g_p, and using Eq. (9) in the narrow well limit, we find for $(\xi/2D)\ln(1/g_p) \ll 1$

$$\phi_p \approx \frac{\tau}{1 + 6(\xi\tau/D)\ln(1/g_p)}. \tag{10}$$

Besides confirming that the structure of the square-well fluid affects ϕ_p only through the stickiness, Eq. (10) also makes it explicit that the locus of the conductor-insulator transition depends (although only logarithmically) on the insulating matrix through g_p, in contrast to the usual continuum percolation theory which predicts a percolation threshold ϕ_c independent of the matrix conductivity.[20]

V. CRITICAL PATH APPROXIMATION

Although colloidal dispersions of tunneling connected particles are intrinsically non-percolative systems, concepts, and quantities of percolation theory are nevertheless at the basis of the CPA (Ref. 33) which, as already shown for HS fluids of conducting particles,[20,22] can reproduce to a high accuracy the tunneling conductivity behavior of composites.

As we have seen in Sec. IV, for sufficiently small ξ/D the EMA conductance g^* is dominated by a characteristic length, x^*, such that the cumulative coordination number satisfies Eq. (7). In a similar way, CPA amounts to approximating the tunneling network conductivity by

$$\sigma \simeq \sigma_0 \exp\left[-\frac{2\delta_c(\phi)}{\xi}\right], \tag{11}$$

where σ_0 is a ϕ-independent conductivity prefactor and $\delta_c(\phi) = r_c(\phi) - D$ is a critical distance given by the shortest among the $\delta_{ij} = r_{ij} - D$ lengths such that the subnetwork defined by all distances $\delta_{ij} \le \delta_c(\phi)$ forms a percolating cluster. From Eq. (11), we see that CPA expresses σ in terms of a critical connectivity distance, $\delta_c(\phi)$, which is a genuine percolation quantity. However, contrary to the continuum percolation approach with fixed connectivity length, in CPA the critical connectivity changes as ϕ and the potential profile are varied. This adaptation of the connectivity range compensates for the artificial basis of the sharp cutoff at δ_c.

To calculate $\delta_c(\phi)$, we follow the route described in Ref. 22. Namely, for fixed ϕ and potential profile, we coat each sphere with a concentric penetrable shell of thickness $\delta/2$, and consider two spheres as connected if their penetrable shells overlap. A clustering algorithm described in Ref. 22 allows computation of the spanning probability $P(\delta)$, which is plotted in Fig. 6 for $\lambda = 1.05$, $\tau = 0.2$, $N = 2000$, and for different values of ϕ. Note that there is a rather sudden change in the slope of $P(\delta)$ when δ/D crosses $\lambda - 1$ (vertical dashed line) which is due to the discontinuity of the square well potential at $r/D = \lambda$.

In order to define a suitable criterion to extract δ_c from the $P(\delta)$ curves for all parameter values used, and which is also insensitive to the feature at $\delta/D = \lambda - 1$, we have carried out the finite-size scaling analysis of the type shown in shown in Fig. 7, where $P(\delta)$ is compared with the percolation probability $P(\phi)$ calculated as a function of ϕ for fixed δ. In Fig. 7(a), we show the evolution of $P(\phi)$ as the system size L/D increases for $\lambda = 1.05$ and $\delta/D = \lambda - 1 = 0.05$. By using the finite-size scaling relation $\phi_c - \phi_c(L) \propto L^{-1/\nu}$, where $\nu \simeq 0.88$ is the correlation length exponent and $\phi_c(L)$ is such

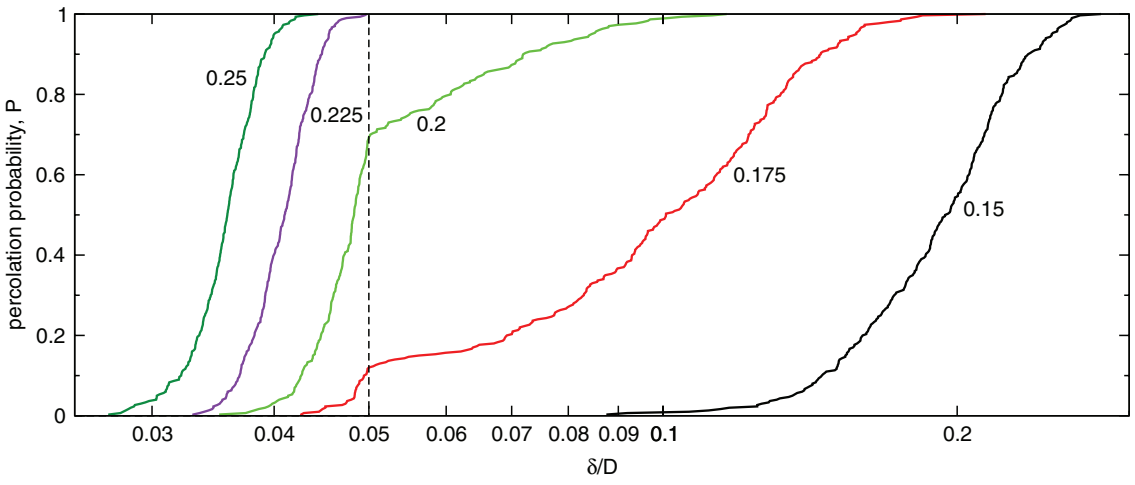

FIG. 6. Percolation probability as a function of the connectivity distance δ for various values of the volume fraction ϕ and for a square-well potential with $\lambda = 1.05$ and $\tau = 0.2$ (i.e., $\epsilon^* = 2.169$). The number of conducting spheres is fixed at $N = 2000$. The vertical dashed line indicates $\delta/D = \lambda - 1$.

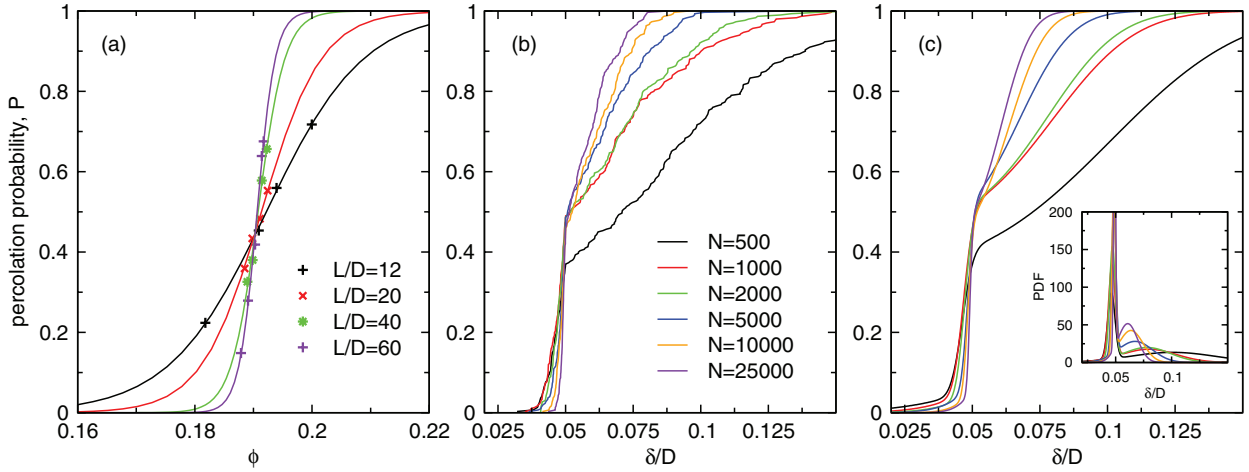

FIG. 7. Percolation probability P for $\lambda = 1.05$ and $\tau = 0.2$ (i.e., $\epsilon^* = 2.169$). (a) P as a function of ϕ for δ/D fixed at $\lambda - 1 = 0.05$ and for different sizes L of the cubic box. (b) P as function of δ/D for $\phi = 0.19$ and for different number N of spheres. (c) Fits of the percolation probability of (b) obtained by using a linear combination of two error functions. Inset: probability distribution function PDF obtained from $dP(\delta)/d\delta$.

that $P = 1/2$, we find that the percolation threshold as $L/D \to \infty$ is $\phi_c = 0.19035 \pm 0.00001$. In Fig. 7(b), we plot $P(\delta)$ obtained for different numbers N of particles by using $\phi = 0.19$. Note that as N increases, the change of slope of $P(\delta)$ at $\delta/D = \lambda - 1 = 0.05$ tends to decrease. This is more clearly seen in Fig. 7(c), where we plot fits of $P(\delta)$ with linear combinations of two error functions, and in the inset where we show the resulting probability distribution function (PDF) $dP(\delta)/d\delta$, which is characterized by two peaks of different strengths. If we use the criterion that $\delta_c(N)$ is given by $P = 1/2$, we find from $\delta_c - \delta_c(N) \propto N^{-1/3\nu}$ that $\delta_c/D = 0.05066 \pm 0.00007$ at $N \to \infty$, practically coinciding with $\delta/D = 0.05$ of Fig. 7(a). Furthermore, for $N = 2000$ the criterion $P = 1/2$ gives $\delta_c/D \simeq 0.0512$, which is only 1% larger than the critical distance at $N \to \infty$.

From the finite-size study of Fig. 7, and from other cases we have considered, we thus see that $P(\delta_c) = 1/2$ is a reliable criterion to find the critical distance even for $N = 2000$. When we compare in Fig. 1 the CDF of the network conductivity with $P_{\rm CPA}(\sigma)$ obtained from $P(\delta)$ by using the CPA expression $\sigma = \sigma_0 \exp(-2\delta/\xi)$ with $\sigma_0 = 0.09$ (thin dashed lines), we see that the shapes of the two probability functions are very similar, which justifies the criterion $P(\sigma) = 1/2$ that we have adopted for the network conductivity results shown in Figs. (2) and (3).

Let us now discuss the conductivity dependence on ϕ and on the potential profile in terms of the CPA formula (11). The calculated values of the critical distance are shown in Fig. 8 for the same parameter values as Figs. 2 and 3. For all cases studied, δ_c is a monotonically decreasing function of ϕ, which is to be expected because larger particle concentrations bring about shorter mean inter-particle distances. However, the rate of decrease depends on whether δ_c/D is greater or less than $\lambda - 1$ (horizontal dashed lines in Fig. 8), which reflects the existence of the two different regions of the conductivity already discussed in Sec. IV. In particular, as shown in Fig. 8(c), when $\delta_c/D \gtrsim \lambda - 1$ the critical distance is governed solely by the particle stickiness and closely follows the AHS

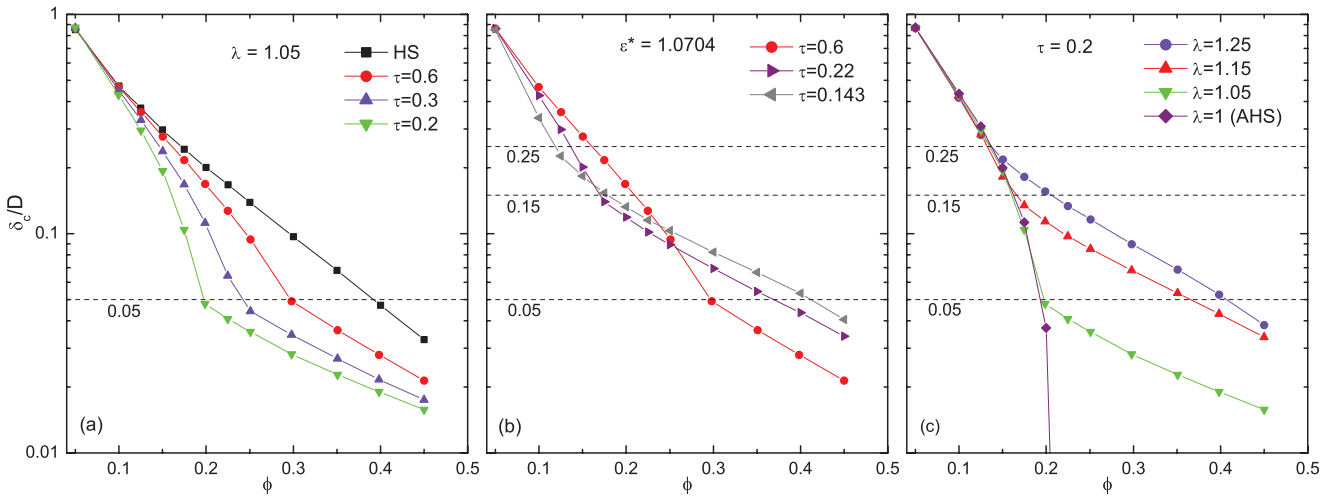

FIG. 8. Calculated critical distance δ_c as a function of ϕ for (a) $\lambda = 1.05$ and different well depths; (b) $\epsilon^* = 1.0704$ and $\lambda = 1.05$, 1.15, and 1.25; (c) λ and ϵ^* varying with $\tau = 0.2$ fixed. The horizontal dashed lines identify $\delta_c/D = \lambda - 1$.

limit, in full correspondence with the low-ϕ behavior of σ of Fig. 3. Indeed when the $\delta_c(\phi)$ values of Fig. 8 are inserted in Eq. (11), we find that the resulting CPA conductivity (plus signs in Figs. 2 and 3) is in excellent agreement with our MC values.[34]

We therefore see that, in analogy with the results of Sec. IV, the conductivity changes driven by attraction are due to the variations of the dominant tunneling distances, which are represented by the effective connectivity length δ_c. From Eq. (11), we see also that in the presence of a finite conductivity σ_p of the insulating matrix, tunneling dominates the overall conductivity as long as $\delta_c(\phi) \lesssim \delta_c(\phi_p)$, where $\delta_c(\phi_p) = (\xi/2)/\ln(\sigma_0/\sigma_p)$ is the connectivity at the insulator-conductor transition.

VI. CONCLUSIONS

In this article, we have studied by theory and simulations the effects of short-range particle attractions on the functional dependencies of the conductivity σ of equilibrium dispersions of conducting spherical fillers electrically connected through tunneling processes. Instead of employing the traditional continuum percolation approach in which a fixed connectivity length is introduced to mimic the extent of the tunneling electron transfer, we have solved the network equations by treating each conducting particle as being connected to all others by tunneling conductances. We have shown that the lack of a fixed connectivity distance gives rise to new and important features which the continuum percolation approach fails to predict, and which could be crucial in the design of nanocomposite materials with unique electrical properties.

In particular, we have found that the conductivity at intermediate and large contents of the conducting fillers is extremely sensitive to the profile of the attractive potential, while the low-density regime is generally governed only by the stickiness of the attraction. As a consequence, materials with similar values of the conductor-insulator concentration ϕ_p may display at $\phi > \phi_p$ conductivities which differ by several orders of magnitude if the attraction is tuned while keeping the stickiness constant. More generally, we have demonstrated that the knowledge of ϕ_p and of its dependence on the attraction are not sufficient conditions to presume the overall behavior of σ as a function of ϕ, in striking contrast to the percolation transition approach represented by Eq. (1).

As discussed in Sec. IV our simulation results can be reproduced by using a recently developed effective medium theory which, for sufficiently small values of ξ/D, expresses the conductivity in terms of the radial distribution function at contact, explicitly relating the different regimes of conduction to the depth and range of the potential well. Furthermore, we have shown how the critical path approximation overcomes the limitations of the continuum percolation approach by allowing the connectivity length to adjust for given ϕ and potential profile, so as to represent the dominant tunneling distances governing σ.

Although we are not aware of experiments on conducting colloidal composites where the electronic conductivity is tuned by controlling the filler attraction,[35] our work may nevertheless stimulate experiments in this direction. In principle, our predictions may be systematically tested in experiments by changing the size and concentration of depletants in colloidal conductors. In particular, we have predicted that an optimal enhancement of the conductivity can be realized by high concentrations of depletants with small sizes compared to those of the conducting particles, so to drive the system towards the AHS limit. Furthermore, stronger enhancements are expected in composites with conducting filler sizes sufficiently large compared to the tunneling decay length ξ, so as to avoid a smearing out of the attraction potential well.

We conclude by pointing out that the system considered here, i.e., attracting fillers with spherical shapes, has served primarily to illustrate the general principles at the basis of the interplay between attraction and tunneling. Stronger effects of the attraction are expected when the conducting particles have shape anisotropy, as in fibrous or plate-like fillers, where the mutual orientations of the particles couple with the attraction interaction. This represents certainly an issue of great interest for future investigations.

ACKNOWLEDGMENTS

B.N. acknowledges support by the Swiss National Science Foundation (Grant No. 200020-135491). M.A.M. is supported by EPSRC (U.K.).

[1] W. Bauhofer and J. Z. Kovacs, Compos. Sci. Technol. **69**, 1486 (2009).
[2] T. Kuilla, S. Bhadra, D. Yao, N. H. Kim, S. Bose, and J. H. Lee, Prog. Polym. Sci. **35**, 1350 (2010).
[3] J. C. Grunlan, W. W. Gerberich, and L. F. Francis, Polym. Eng. Sci. **41**, 1947 (2001).
[4] A. V. Kyrylyuk, M. C. Hermant, T. Schilling, B. Klumperman, C. E. Koning, and P. van der Schoot, Nat. Nanotechnol. **6**, 364 (2011).
[5] B. Vigolo, C. Coulon, M. Maugey, C. Zakri, and P. Poulin, Science **309**, 920 (2005).
[6] S. B. Kharchenko, J. F. Douglas, J. Obrzut, E. A. Grulke, and K. B. Migler, Nature Mater. **3**, 564 (2004).
[7] M. C. Hermant, B. Klumperman, A. V. Kyrylyuk, P. van der Schoot, and C. E. Koning, Soft Matter **5**, 878 (2009).
[8] D. Stauffer and A. Aharony, *Introduction to Percolation Theory* (Taylor & Francis, London, 1994).
[9] M. Sahimi, *Heterogeneous Materials I. Linear Transport and Optical Properties* (Springer, New York, 2003).
[10] S. Vionnet-Menot, C. Grimaldi, T. Maeder, S. Strässler, and P. Ryser, Phys. Rev. B **71**, 064201 (2005).
[11] I. Balberg, C. H. Anderson, S. Alexander, and N. Wagner, Phys. Rev. B **30**, 3933 (1984).
[12] R. H. J. Otten and P. van der Schoot, Phys. Rev. Lett. **103**, 225704 (2009); J. Chem. Phys. **134**, 094902 (2011).
[13] A. P. Chatterjee, J. Chem. Phys. **132**, 224905 (2010).
[14] R. P. Kusy, J. Appl. Phys. **48**, 5301 (1977).
[15] N. Johner, C. Grimaldi, T. Maeder, and P. Ryser, Phys. Rev. E **79**, 020104(R) (2009).
[16] Y. C. Chiew and E. D. Glandt, J. Phys. A: Math. Gen. **16**, 2599 (1983).
[17] A. L. R. Bug, S. A. Safran, G. S. Grest, and I. Webman, Phys. Rev. Lett. **55**, 1896 (1985); S. A. Safran, I. Webman, and G. S. Grest, Phys. Rev. A **32**, 506 (1985).
[18] T. Schilling, S. Jungblut, and M. A. Miller, Phys. Rev. Lett. **98**, 108303 (2007).
[19] A. V. Kyrylyuk and P. van der Schoot, Proc. Natl. Acad. Sci. U.S.A. **105**, 8221 (2008).
[20] G. Ambrosetti, C. Grimaldi, I. Balberg, T. Maeder, A. Danani, and P. Ryser, Phys. Rev. B **81**, 155434 (2010).
[21] G. Ambrosetti, I. Balberg, and C. Grimaldi, Phys. Rev. B **82**, 134201 (2010).
[22] B. Nigro, G. Ambrosetti, C. Grimaldi, T. Maeder, and P. Ryser, Phys. Rev. B **83**, 064203 (2011).

[23]H. N. W. Lekkerkerker and R. Tuinier, *Colloids and the Depletion Interaction* (Springer, Dordrecht, 2011).
[24]R. J. Baxter, J. Chem. Phys. **49**, 2770 (1968).
[25]M. G. Noro and D. Frenkel, J. Chem. Phys. **113**, 2941 (2000).
[26]G. Foffi and F. Sciortino, Phys. Rev. E **74**, 050401(R) (2006).
[27]J. Largo, M. A. Miller, and F. Sciortino, J. Chem. Phys. **128**, 134513 (2008).
[28]M. A. Miller and D. Frenkel, J. Chem. Phys. **121**, 535 (2004).
[29]Note that in practice σ_p may also be given by the lowest measurable conductivity which depends on the experimental setup.
[30]C. Grimaldi, Europhys. Lett. **96**, 36004 (2011).
[31]S. B. Yuste and A. Santos, J. Chem. Phys. **101**, 2355 (1994).
[32]J. Largo, J. R. Solana, S. B. Yuste, and A. Santos, J. Chem. Phys. **122**, 084510 (2005).
[33]V. Ambegaokar, B. I. Halperin, and J. S. Langer, Phys. Rev. B **4**, 2612 (1971); B. I. Shklovskii and A. L. Efros, Sov. Phys. JETP **33**, 468 (1971).
[34]The values of the prefactor σ_0 which best fit the MC data lie between 0.08 and 0.1, i.e., they are almost independent of the potential profile.
[35]In Ref. 5, attraction between nanotubes was tuned by means of depletion interaction induced by micelles of ionic surfactants. Since the resulting solvent was a conductive electrolyte, the dc conductivity provided no useful information and only the effects of attraction on the dielectric constant were measured.